Electronic Supplementary Material (ESI) for Journal of Materials Chemistry A.
This journal is © The Royal Society of Chemistry 2022

Supporting Information

Density functional theory study of two-atom active site transition-metal/iridium electrocatalyst for ammonia synthesis

Wei Song[a], Zhe Fu[e], Xiao Liu[a], Yongliang Guo[a], Chaozheng He[b,c]*, Ling Fu[d]*

[a]*School of Science, Henan Institute of Technology, Xinxiang, 453003, P.R. China*

[b]*School of Materials Science and Chemical Engineering, Xi'an Technological University, Xi'an, 710021, P. R. China*

[c]*Institute of Environmental and Energy Catalysis, School of Materials Science and Chemical Engineering, Xi'an Technological University, Xi'an, 710021, P. R. China*

[d]*College of Resources and Environmental Engineering, Tianshui Normal University, Tianshui, 741001, P.R. China*

[e]*Department of Electronic Communication Engineering, Xinxiang University, Xinxiang, 453003, P.R. China*

***Corresponding authors:**

E-mail: ful263@nenu.edu.cn (L. Fu); hecz2019@xatu.edu.cn (C. He)

Table S1 The formation energy (E_f in eV) of two TM (TM=Ti–Zn) atoms doped Ir(100).

	E_f (eV)	E_{coh} (eV)	ΔE (eV)
Ti_2@Ir(100)-para	–14.322	–6.303	–8.019
V_2@Ir(100)-para	–14.034	–7.287	–6.747
Cr_2@Ir(100)-para	–11.115	–6.753	–4.362
Mn_2@Ir(100)-para	–6.231	–4.462	–1.769
Fe_2@Ir(100)-para	–8.288	–5.609	–2.679
Co_2@Ir(100)-para	–9.640	–6.132	–3.508
Ni_2@Ir(100)-para	–9.520	–5.732	–3.788
Cu_2@Ir(100)-para	–6.269	–4.218	–2.051
Zn_2@Ir(100)-para	–2.669	–0.233	–2.436
Ti_2@Ir(100)-ortho	–14.099	–6.303	–7.796
V_2@Ir(100)-ortho	–13.766	–7.287	–6.479
Cr_2@Ir(100)-ortho	–10.881	–6.753	–4.128
Mn_2@Ir(100)-ortho	–6.191	–4.462	–1.729
Fe_2@Ir(100)-ortho	–8.312	–5.609	–2.703
Co_2@Ir(100)-ortho	–9.854	–6.132	–3.722
Ni_2@Ir(100)-ortho	–9.787	–5.732	–3.955
Cu_2@Ir(100)-ortho	–6.453	–4.218	–2.235
Zn_2@Ir(100)-ortho	–2.857	–0.233	–2.624

Table S2 The N–N bond length ($d_{N\text{-}N}$ in Å) and adsorption energy (E_{ads} in eV) of N_2 on different sites of TM_2@Ir(100)-para (TM= Ti, V, Cr, Mn, and Fe).

S1 site	$d_{N\text{-}N}$ (Å)	E_{ads} (eV)	S2 site	$d_{N\text{-}N}$ (Å)	E_{ads} (eV)
Ti	—	—	Ti	1.180	–0.765
V	—	—	V	1.182	–0.822
Cr	—	—	Cr	1.180	–1.002
Mn	—	—	Mn	1.178	–0.888
Fe	—	—	Fe	1.175	–1.398
S3 site	**$d_{N\text{-}N}$ (Å)**	**E_{ads} (eV)**	S4 site	$d_{N\text{-}N}$ (Å)	E_{ads} (eV)
Ti	**1.278**	**–1.431**	Ti	1.175	–0.306
V	**1.287**	**–1.370**	V	1.172	–0.273
Cr	**1.292**	**–1.334**	Cr	1.164	–0.485
Mn	**1.289**	**–1.270**	Mn	1.135	–0.513
Fe	**1.286**	**–1.123**	Fe	1.135	–1.188
S5 site	$d_{N\text{-}N}$ (Å)	E_{ads} (eV)			
Ti	1.140	–1.201			
V	1.137	–1.143			
Cr	1.137	–1.428			
Mn	1.132	–1.332			
Fe	1.135	–1.587			

Table S3 The N–N bond length ($d_{N\text{-}N}$ in Å) and adsorption energy (E_{ads} in eV) of N_2 on different sites of TM_2@Ir(100)-ortho (TM= Mn, Fe, Co, Ni, Cu, and Zn).

S1 site	$d_{N\text{-}N}$ (Å)	E_{ads} (eV)	S2 site	$d_{N\text{-}N}$ (Å)	E_{ads} (eV)
Mn	1.242	–1.761	Mn	—	—
Fe	1.235	–1.208	Fe	1.168	–1.514
Co	1.208	–0.498	Co	1.164	–0.742
Ni	1.218	–0.384	Ni	1.160	–0.483
Cu	1.176	–0.556	Cu	1.137	–0.066
Zn	1.176	–0.611	Zn	1.118	–0.157
S3 site	$d_{N\text{-}N}$ (Å)	E_{ads} (eV)	**S4 site**	**$d_{N\text{-}N}$ (Å)**	**E_{ads} (eV)**
Mn	1.176	–0.915	**Mn**	**1.290**	**–1.451**
Fe	1.172	–0.862	**Fe**	**1.283**	**–1.282**
Co	1.168	–0.484	**Co**	**1.277**	**–0.764**
Ni	1.167	–0.477	**Ni**	**1.266**	**–0.725**
Cu	1.135	–0.996	**Cu**	**1.255**	**–0.319**
Zn	1.135	–1.025	**Zn**	**1.259**	**–0.088**
S5 site	$d_{N\text{-}N}$ (Å)	E_{ads} (eV)	S6 site	$d_{N\text{-}N}$ (Å)	E_{ads} (eV)
Mn	—	—	Mn	1.132	–1.386
Fe	—	—	Fe	—	—
Co	—	—	Co	—	—
Ni	1.263	–0.657	Ni	—	—
Cu	1.241	–0.169	Cu	—	—
Zn	1.240	–0.101	Zn	—	—
S7 site	$d_{N\text{-}N}$ (Å)	E_{ads} (eV)	S8 site	$d_{N\text{-}N}$ (Å)	E_{ads} (eV)
Mn	1.131	–1.993	Mn	1.188	–1.440
Fe	1.137	–1.749	Fe	1.133	–1.886
Co	1.135	–0.972	Co	—	—
Ni	1.130	–0.793	Ni	1.132	–0.790
Cu	1.126	–0.368	Cu	1.135	–0.996
Zn	1.118	–0.156	Zn	1.135	–1.024

Notes: "—" means that N_2 cannot be stably adsorbed at this site or has been adsorbed to other sites.

Table S4 Total magnetic moment (M in μ_B) of Mn_2@Ir(100) and Fe_2@Ir(100) .

	Mn_2@Ir(100)-para	Mn_2@Ir(100)-ortho	Fe_2@Ir(100)-para	Fe_2@Ir(100)-ortho
M (in μ_B)	2.927	3.423	2.699	1.162

Table S5 The adsorption energy (E_{ads} in eV), Bader charge (Q in e) and N–N bond length ($d_{N\text{-}N}$ in Å) of N_2 on Mn_2@Ir(100)-para using DFT and DFT+U calculation, respectively.

Mn_2@Ir(100)-para	E_{ads} (eV)	Q (e)	$d_{N\text{-}N}$ (Å)
DFT	–1.270	1.167	1.289
DFT+U	–1.201	1.165	1.285

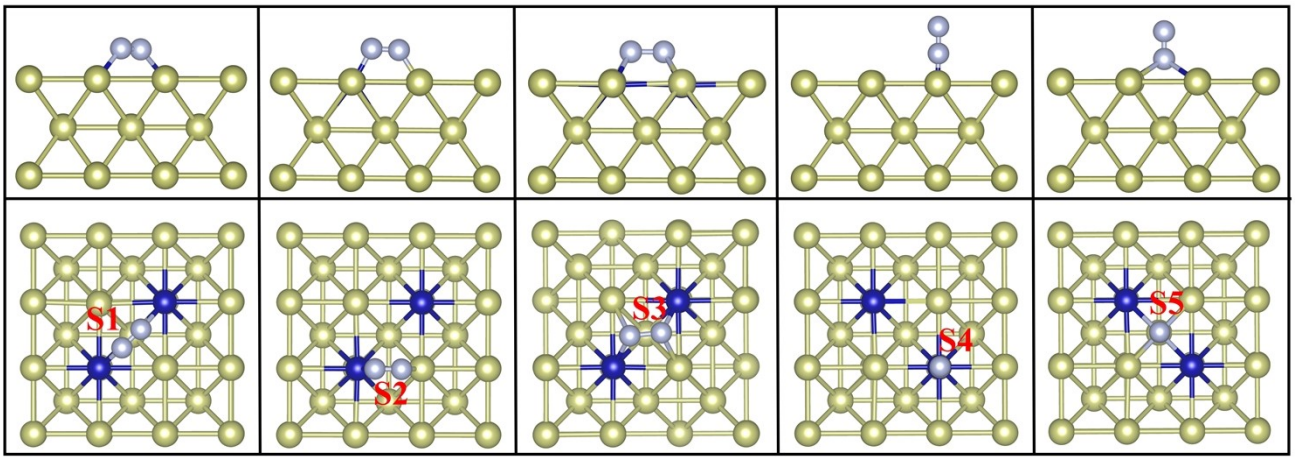

Fig. S1. Side and top view of N_2 adsorption on different sites of TM_2@Ir(100)-para.

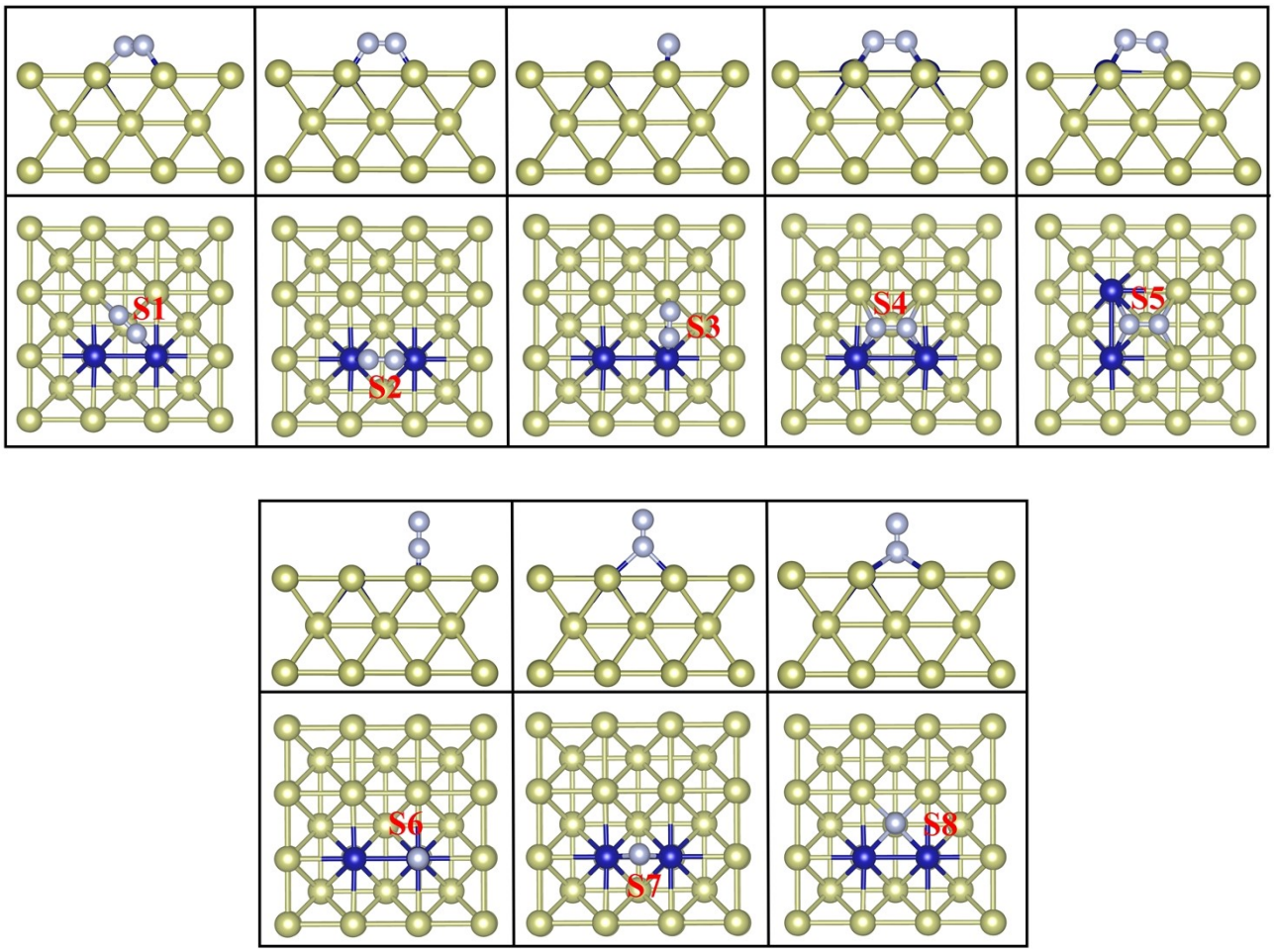

Fig. S2. Side and top view of N_2 adsorption on different sites of TM_2@Ir(100)-ortho.

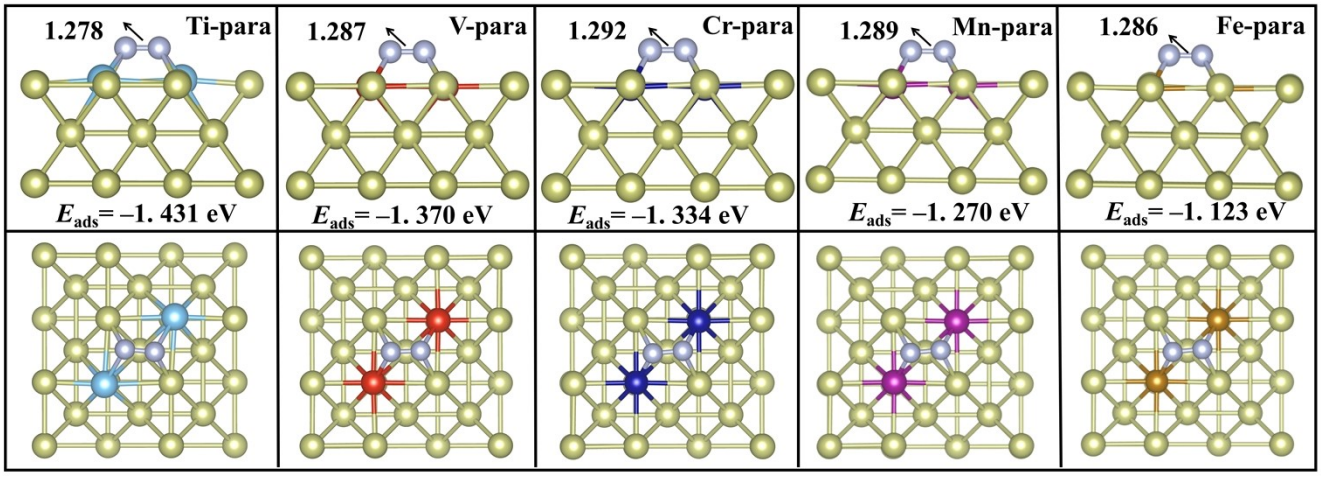

Fig. S3. The most stable structures and corresponding adsorption energy (E_{ads} in eV) as well as N–N bond length ($d_{N\text{-}N}$ in Å) of N_2 adsorption on TM_2@Ir(100)-para (TM= Ti, V, Cr, Mn, and Fe).

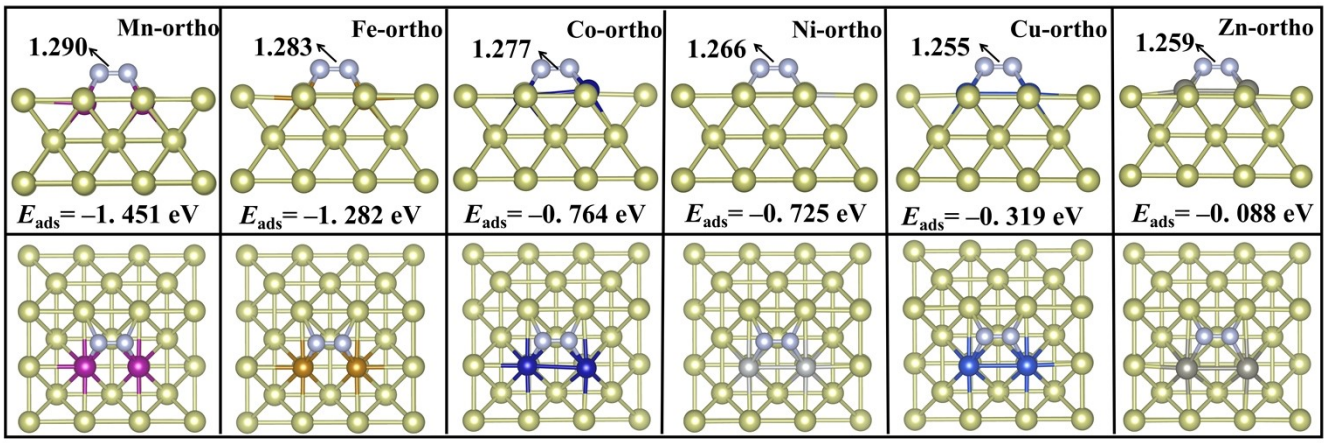

Fig. S4. The most stable structures and corresponding adsorption energy (E_{ads} in eV) as well as N–N bond length ($d_{N\text{-}N}$ in Å) of N_2 adsorption on TM_2@Ir(100)-ortho (TM= Mn, Fe, Co, Ni, Cu, and Zn).

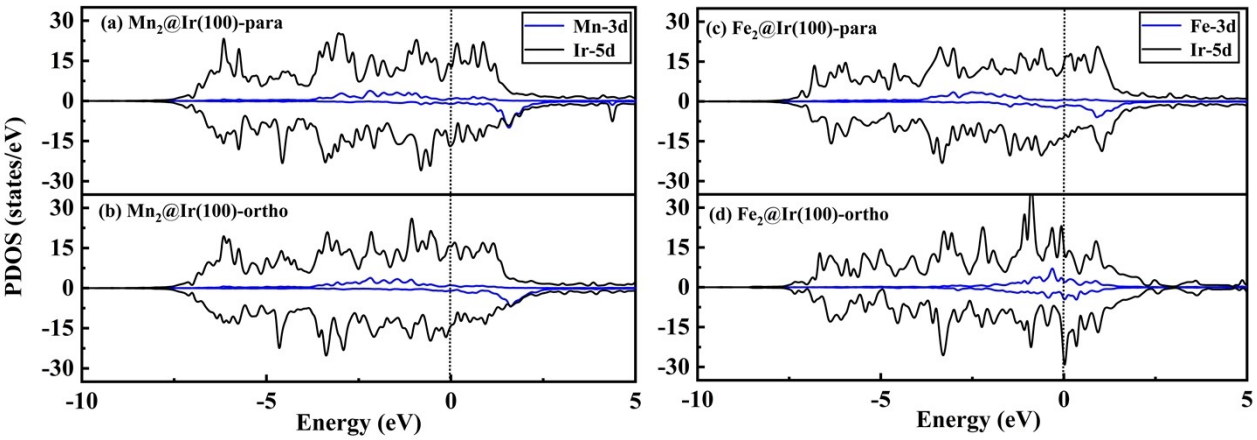

Fig. S5. The calculated partial density of states (PDOS) of (a) Mn_2@Ir(100)-para, (b) Mn_2@Ir(100)-ortho, (c) Fe_2@Ir(100)-para, and (d) Fe_2@Ir(100)-ortho, respectively. The Fermi level is set to zero in the dotted line.

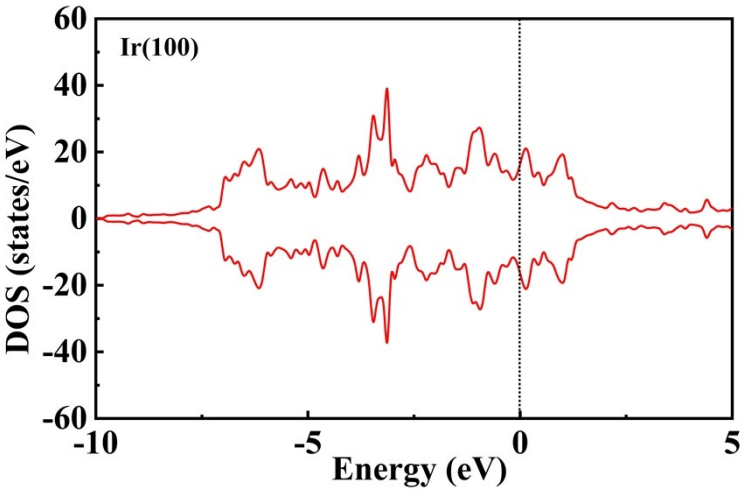

Fig. S6. The calculated density of states (DOS) of Ir(100). The Fermi level is set to zero in the dotted line.

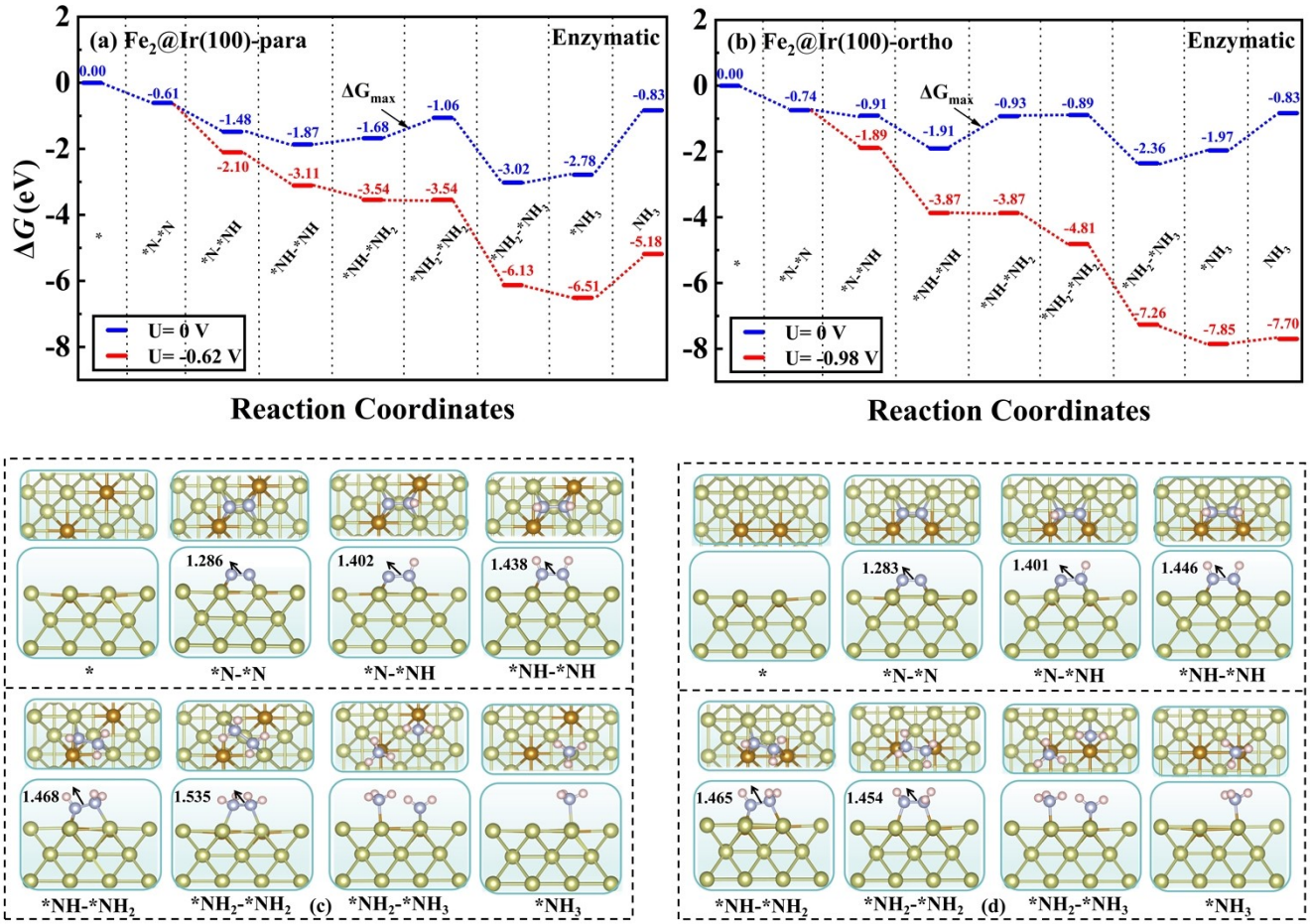

Fig. S7. Gibbs free energy diagrams of the NRR process at zero (blue lines) and applied potential (red lines) of various reaction intermediates adsorption on (a) Fe_2@Ir(100)-para and (b) Fe_2@Ir(100)-ortho via the enzymatic pathway; (c) and (d) the corresponding optimized geometric structures, respectively.

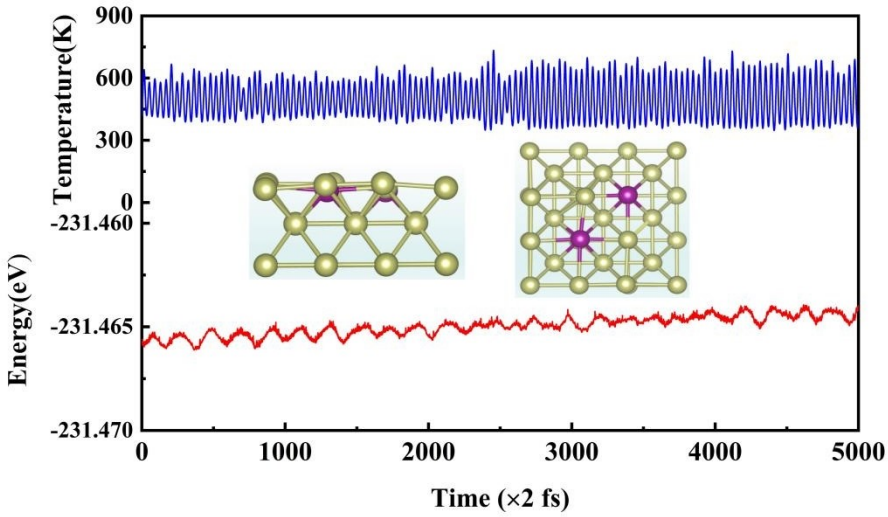

Fig. S8. The temperature and energy fluctuations of Mn_2@Ir(100)-para during 10ps of AIMD simulation. The insets illustrate the top and side view of Mn_2@Ir(100)-para after 10ps AIMD simulation at T = 500K.

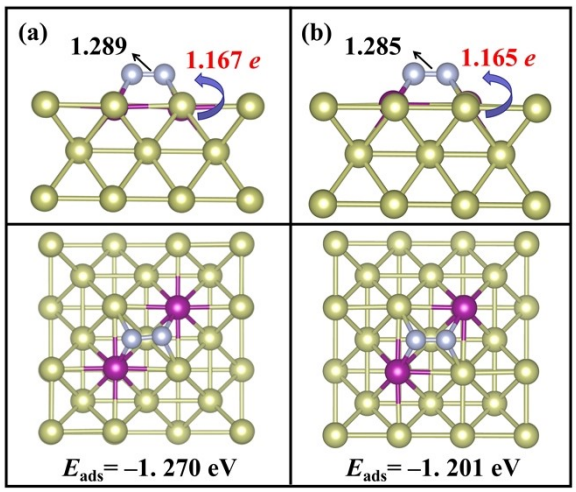

Fig. S9. The optimized adsorption structures of N_2 on Mn_2@Ir(100)-para using (a) DFT and (b) DFT+U calculation.